RSC Advances

ROYAL SOCIETY OF CHEMISTRY

www.rsc.org/advances

Stainless steel felt as diffusion backing for high-performance microbial fuel cell cathodes

Zhaozheng Qiu, Liling Wei*, Gang Wang, Min Su, Jianquan Shen *

Beijing National Laboratory for Molecular Sciences (BNLMS), Key Laboratory of Green Printing, Institute of Chemistry, Chinese Academy of Sciences, , Beijing 100190, China

*Corresponding author

Address: Institute of Chemistry, Chinese Academy of Sciences, Zhongguancun North First Street 2, Beijing 100190, PR China.

Tel.: +86 10 61934539; fax: +86 10 62559373.

E-mail address: weill@iccas.ac.cn; jqshen@iccas.ac.cn

Abstract

Novel three-dimensional (3D) macroporous cathodes for microbial fuel cells (MFCs) are constructed by using stainless steel felt (SSF) as the diffusion backing and the current collector, instead of those two-dimensional (2D) materials such as carbon cloth (CC) or stainless steel mesh (SSM), thereby resulting in an enlarged surface area for oxygen reduction reaction (ORR). Different amounts of carbon black (CB) are applied in the base layer to optimize the performance of those SSF cathodes. The MFCs using the SSF cathodes with CB loading of 1.56 mg cm^{-2} (SSF-1.56) achieve a maximum power density of 1315 ± 6 mW m^{-2}, which is 60% and 42% higher than those using the CC and SSM cathodes, respectively. The results show that the cathode of SSF-1.56 exhibits an excellent catalytic activity for ORR as well as a reduced total

internal resistance, thanks to the improved three-phase interface (TPI) that not only facilitates the electron transfer, the proton transfer and the oxygen diffusion, but also offers a large surface for ORR at the cathode. Our research also demonstrates that the SSF cathodes with an optimal CB loading will benefit the advancement of MFCs in practical application.

Keywords: Microbial fuel cell; Cathode; Stainless steel felt; Carbon black

1. Introduction

Microbial fuel cells (MFCs), using electro-active micro-organisms as catalysts, directly convert chemical energy of organic or inorganic matter into electrical energy [1]. One of the potential applications of the MFC technology is wastewater treatment, where electrical energy is simultaneously recovered as the wastewater is treated, which is the main advantage of this technology over other conventional methods in the field [2]. Although such oxidants as ferricyanide [3], nitrate [4] and permanganate [5] have been adopted as electron acceptors at the cathodes in MFCs, oxygen, as a cost-effective, sustainable and environmental friendly oxidant, is the most promising one for wastewater treatment applications [6]. Owing to its simple structure, low cost and direct use of oxygen in ambient air, the air-cathode MFC is highly efficient and considered to be of the greatest potential for practical applications [7].

At present time, the MFC performance of electricity generation still can't satisfy the needs of practical applications. The main challenges for the development of the

MFC technology lie in how to further improve the power production and the electrons recovery from the substrate, while at the same time reduce costs of the materials for MFCs' commercialization [7]. According to some previous researches, the cathodic performances and the cathode surface area have been proved to be the two most important factors that affect the performances of MFCs in the process of scaling-up [6, 8-11]. Meanwhile the expenses of cathode materials account for a large part in the total MFC costs [12]. Therefore, exploiting cost-effective cathode materials and designing efficient cathodes to improve the performances of MFCs emerge as the main issues in the practical applications of MFCs.

Nowadays, most laboratories adopt carbon cloth (CC) as the backing of air-cathodes [13, 14]. But, due to its low mechanical strength and the large resistance as the reactor size increases, the CC cathodes seem impracticable for scaled-up MFCs. Stainless steel mesh (SSM), which is inexpensive, widely available, mechanically strong and relatively anticorrosive [15, 16], is also adopted as the current collector and the backing for air-cathodes so that the electrode ohmic losses can be reduced. It has been reported that a maximum power density of 1610 ± 56 mWm^{-2} was obtained in a small lab-scale reactor by using SSM as the current collector and the backing [6]. Further research has shown that the size of mesh openings exert a significant effect on the performances of cathodes, which were primarily limited by oxygen reduction kinetics rather than the mass transfer [16].

However, because of their limited interfacial channels for oxygen and proton transport as well as the restricted surface area for oxygen reduction reaction (ORR),

the cathodes using the two-dimensional (2D) CC and SSM prevent the power output from further increasing. The restricted reactive surface area and high activation energy barrier lead to the activated loss of electrodes, while the flat structure and the relatively lower porosity result in the diffusion limitation of these electrodes [17]. One of the effective ways to eliminate those above-mentioned drawbacks is to employ porous three-dimensional (3D) electrodes, bearing such advantages as a large surface area for reaction, efficient interfacial transport, shortened diffusion paths and reduced activated and/or diffusion resistance. Stainless steel felt (SSF), a commercially available and inexpensive 3D porous filter material widely used for gas and liquid filtration, whose open 3D macroporous structure enables a large specific surface area, high anticorrosion, excellent mechanical strength and uniform aperture distribution [18], is considered to be an ideal backing and current collector for the air-cathode design in MFCs. A recent report has demonstrated that the MFC using a graphene modified SSF anode has produced a maximum power density of 2142 mW m^{-2} , which was attributed to its large surface area for reaction, excellent interfacial transport and biocompatible interface for bacterial colonization [17]. Guo et al[19] has put forward a simple method to make biocompatible SSF anodes by mere flame oxidation, proved to be rapid, energy-efficient and satisfactory for the large-scale anode fabrication. To our knowledge, up till now there has been no report on the application of the material in MFC cathodes, although SSF has been tested as the gas diffusion layer in proton exchange membrane fuel cells (PEMFCs) [20] and as the cathode diffusion backing and the current collector for a micro direct methanol fuel cell [21].

Carbon black (CB) is primarily used in Pt cathodes as the catalyst support and the base layer stuffing due to its high electrical conductivity. But, the optimal amount of CB in the base layer has not been determined, and it is important for us to have a clear idea of the impact of CB loading on cathode performance. As illustrated by one report, CB loadings significantly affect the performances of activated carbon cathodes [22], we have varied the loadings of CB particles in the base layer during the cathode fabrication in order to improve the performances of the SSF based cathodes. Therefore, the aims of this study are to fabricate air-cathodes by using open 3D macroporous SSF as the diffusion backing and the current collector and to determine the impact of CB loadings in the base layer on the cathode performances in both electrochemical and MFC tests.

2. Materials and methods

2.1. Cathode fabrication

The cathodes fabricated here are based on integrating the backing (SSF), the catalyst (Pt), and the diffusion layer (polytetrafluoroethylene PTFE) into one single cathode structure, among which SSF (316L-40, 0.7 mm thick) was purchased from Xi'an Filter Metal Materials Co., Ltd with the mean filter rating of 40.7 μm and the mean porosity of 78%. The fabrication procedure has been modified from Cheng's method [14]. The SSF substrates were firstly soaked in acetone for 4 hours and then rinsed with deionized water before fabrication. The PTFE/CB base layer was prepared by applying a mixture of CB powder (Alfa Aesar, USA) and PTFE solution (31.2 μL 30 wt % PTFE per square centimeter) onto the air-facing side of the backing material,

air-dried at room temperature for 2 hours, and subsequently heated at 370°C for 30 minutes. The CB loading in the base layer was changed at weight per square centimeter: 0.39 mg, 0.78 mg, 1.56 mg and 3.12 mg. Multiple PTFE DLs containing PTFE solution (60 wt %) were coated on the top of the base layer (3 mg cm^{-2} of PTFE for every coating), followed by being air-dried at room temperature and then heated at 370 °C for 5 minutes. Four DLs of PTFE were applied on the base layer, producing the cathodes of SSF-0.39, SSF-0.78, SSF-1.56 and SSF-3.12, respectively. CC (HCP331N, Hesen, China) and SSM (type SUS-304 SS, 80×80 openings per square inch) were also tested as the cathode backing materials. These two kinds of cathodes, consisting four DLs of PTFE, were prepared following previously described method [14]. The CB loading in those base layers was chosen to be 1.56 mg cm^{-2}, and the cathodes are denoted here as CC-1.56 and SSM-1.56, respectively. When the fabrication of DLs has finished, Pt catalyst (0.2 mg cm^{-2}, 40% Pt Hesen, China) was then applied to the water-facing side of the cathodes as previously described, using Nafion as a binder [23].

2.2. MFC construction and operation

As previously reported, the Plexiglas cylindrical single-chamber MFCs consist of an anode and a cathode in an anode chamber 4 cm in length by 3 cm in diameter (empty bed volume of 28 mL) [14]. The anode electrodes were made of graphite felt (2 cm × 2 cm × 0.5 cm, Beijing Sanye Carbon Co., Ltd). After being soaked in acetone for 4 hours and rinsed with deionized water, the graphite felt was heated at 400 °C for 1 hour. Titanium wire was used to fix the anode and connect the circuit.

Each MFC reactor was inoculated using mixed cultures taken from the anode chamber of a two-chamber MFC for electricity generation, operating in batch mode [3]. All anodes were originally pre-inoculated in a large single-chamber MFC during start-up to ensure that the biofilm on anodes could achieve the identical performance during acclimation. The medium (per liter) applied sucrose as the fuel (1000 mg), and a phosphate buffer solution (PBS) containing NH_4HCO_3, 500 mg; Na_2CO_3, 2000 mg; $NaH_2PO_4 \cdot 2H_2O$, 3978 mg; $Na_2HPO_4 \cdot 12H_2O$, 8771 mg; K_2HPO_4, 125 mg; $MgCl_2 \cdot 6H_2O$, 100 mg; trace minerals (12.5 mL L^{-1}) and vitamins (5 mL L^{-1}) [24]. The minerals contains (per liter): nitrilotriacetic acid, 1.5 g; $MgSO_4 \cdot 7H_2O$, 3.0 g; $MnSO_4 \cdot 2H_2O$, 0.5 g; NaCl, 1.0 g; $FeSO_4 \cdot 7H_2O$, 0.1g; $CaCl_2 \cdot 2H2O$, 0.1g; $CoCl_2$, 0.1 g; $ZnSO_4$, 0.10g; $CuSO_4 \cdot 5H_2O$, 0.01 g; $AlK(SO_4)_2$, 0.01 g; H_3BO_3, 0.01 g; $Na_2MoO_4 \cdot 2H_2O$, 0.01 g and adjust pH to 7.0 with KOH. The initial COD and pH of the anolyte were 1122 mg L^{-1} and 7.70, respectively. MFCs were operated in fed-batch mode at 35 °C.

2.3. Analytics and calculation

Voltage (E) across the external resistor (1000 Ω, except as noted) in the MFC circuit was continuously measured at 5 minute intervals using a data acquisition system (CT-3008-5V50mA-S4, Xinwei, China). Current (I) was calculated by $I = E/R_e$, where R_e represents the external resistance; power (P) was calculated according to $P = IE$ as previously described [2]. Polarization and power density curves were obtained by changing the external resistance from 1000 Ω to 50 Ω in decreasing order, with a time interval of 30 min for each external resistance to ensure a relatively stable voltage can

be achieved. The Coulombic efficiency (CE) was calculated as CE (%) = $C_p/C_t \times 100\%$, where C_p is produced coulombs that calculated by integrating the current over time, and C_t is the theoretical amount of coulombs based on COD removal [2].

Electrochemical properties and impedance behaviors of the cathodes were studied by linear sweep voltammetry (LSV) and electrochemical impedance spectroscopy (EIS) using an electrochemical workstation (CHI 604E, ChenHua Instruments Co., Ltd., Shanghai, China). LSV tests were conducted in the absence of bacteria and substrate, using a three-electrode assembly which consists of a working electrode (cathode with 7 cm^2 projected surface area), a counter electrode (Pt wire) and an Ag/AgCl reference electrode (218, Shanghai REX Instrument Factory). Potential was scanned from 0.4 V to −0.3 V (vs. Ag/AgCl electrode) with the scan rate of −1 mV s^{-1}.

Electrochemical impedance spectroscopy (EIS) was employed to measure the internal resistances of the cathodes at the end of a batch operation. The measurements were conducted at polarized conditions of 0.1 V, 0 V and −0.1 V (vs. saturated Ag/AgCl electrode), which were within the range of the operating potentials of the MFC cathodes, over a frequency range of 100 kHz to 10 mHz with a sinusoidal perturbation of 10 mV amplitude [8]. EIS, applied as a useful electrochemical technology, can be employed to measure the internal resistance (R_{int}) of the cathodes. The Nyquist plots were used to interpret the spectra. The specific composition of each resistance of air-cathodes was determined by using Zview 2.0 software.

For EIS data analysis, two different equivalent circuits were used for the SSF

177 cathodes and the other two cathodes with CC and SSM backing due to the differences
178 in shape of the spectra. Individual components of the internal resistance for the SSF
179 cathodes were identified by fitting their EIS spectra to an equivalent circuit as
180 previously described [16]. This equivalent circuit assumes that the cathode reaction is
181 affected by both reaction kinetics and diffusion. The symbol R_s and R_{ct} represent the
182 solution resistance and the charge transfer resistance, respectively. A constant phase
183 element (Q) was used to model double layer capacitance while a Warburg element (W)
184 was employed to evaluate the diffusion resistance (Fig. 1A). On the other hand, the
185 spectra for the CC and SSM cathodes were fitted into equivalent circuits respectively
186 according to the flooded-agglomerate model [25]. The equivalent circuit is composed of
187 a solution element (solution resistance, R_s) in series with a charge transfer element
188 (charge transfer resistance R_{ct} in parallel with double layer capacitance C_{dl}) and
189 followed by a diffusion element (diffusion resistance R_d in parallel with pore
190 adsorption capacitance C_{ad}) (Fig. 1B).

191 Scanning electron microscopy (SEM) (S-4300, Hitachi, Japan) was used to
192 characterize the transversal surface morphology of the samples. All experiments have
193 been repeated twice and similar results were obtained.

194 **3. Results and discussion**

195 *3.1. Performance of cathodes in MFC tests*

196 Power production performances of different cathodes in MFCs have been examined.
197 Repeatable and stable voltages were immediately obtained in all MFCs due to the use
198 of pre-acclimated anodes. Although there were very small differences in voltage

among these MFCs at a high external resistance of 1 kΩ, the MFC using SSF-1.56 exhibited higher voltage output than the other cathodes (CC-1.56 and SSM-1.56) with the same CB loading of 1.56 mg cm^{-2} (Fig. 2A), while the cathodes of SSF-0.78 and SSF-1.56 produced relatively higher voltages than the other two SSF cathodes (SSF-0.39 and SSF-3.12) (Fig. 2B). Over 3 batch cycles of operation, the average value of the maximum voltages reached 569 ± 10 mV (± S.D., n = 3) for the SSF-1.56 cathodes while the highest values of the CC and SSM cathodes reached 529 ± 7 mV and 526 ± 4 mV, respectively.

At the 4th batch cycle of operation, power densities and electrode potentials have been measured for MFCs with different cathodes. The MFCs equipped with the SSF-1.56 cathodes achieved the highest maximum power density of 1315 ± 6 mW m^{-2} (± S.D., duplicate reactors), 60% and 42% higher than those with the CC and SSM cathodes, respectively. On the other hand, the CC-1.56 cathodes produced the lowest maximum power density of 820 ± 13 mW m^{-2} (Fig. 3A). It was also found out that there were large differences in power production performances of the SSF cathodes with different CB loading in the base layers. The maximum power density was 934 ± 9 mW m^{-2} for the MFCs using SSF cathodes with 0.39 mg cm^{-2} CB loading. When additional CB was applied into the base layers, the maximum power density increased to 1093 ± 25 mW m^{-2} (SSF-0.78) and 1315 ± 6 mW m^{-2} (SSF-1.56). However, further increment of the CB loading reduced the maximum power density, namely 1156 ± 8 mW m^{-2} for SSF-3.12. The cathode potentials followed the same changing trend as the power generation, while the anode potentials were basically the same at

given current densities in all MFCs, indicating the fact that discrepancies in the performances of cathodes lead to the differences in power generation of various MFCs (Fig. 3B).

With the same CB loading of 1.56 mg cm^{-2}, the MFC with the SSF cathodes produced a much higher maximum power density than those with the CC or SSM cathodes, which can be attributed to the improved ORR at three-phase interface (TPI) in the open three-dimensional (3D) macroporous structure of SSF cathodes. Furthermore, the cathodes with different CB loadings in the base layers demonstrated such wide variations in MFC performances that it can be concluded that the amounts of CB blended in base layers exert a significant effect on the performances of cathodes in power generation.

3.2. Performance of cathodes in electrochemical tests

LSV tests were conducted to evaluate the electrochemical performances of different cathodes in the absence of bacteria. The SSF cathodes with different CB loading in the base layers were compared with the CC and SSM cathodes, the results of which showed that the SSF-1.56 cathode exhibited a higher current density than the other cathodes at a given applied potential (Fig. 4). Although the current densities of SSM-1.56 and CC-1.56 were similar at a given applied potential, the onset potential of SSM-1.56 was higher than that of CC-1.56, thereby resulting in a higher maximum power density of SSM-1.56. In our tests, the current densities obtained from the MFCs were in the range of 0–8 A m^{-2}, and the maximum power densities of all MFCs were generally obtained at the cathodic potential around –0.1 V. Thus, although

243 higher current densities were obtained at lower potentials than −0.12 V, the MFCs
244 with the SSF-0.39 cathodes performed poorly in power generation, due to the bad
245 electrochemical performances at higher potential than −0.12 V. The changes in current
246 densities of cathodes in LSV tests demonstrated a similar trend with those in power
247 production which, to a certain degree, enables us to predict the performances of
248 cathodes in MFC tests.

249 *3.3. Morphological characteristics of cathodes' transversal surface*

250 Morphological characteristics of cathodes' transversal surface were observed with
251 SEM. As shown in Fig. 5C and D, the cathodes made from CC and SSM have few
252 porous diffusion paths. SSF made of pressed stainless steel fiber of ~20 μm in
253 diameter, on the contrary, forms a relatively uniform macroporous 3D configuration,
254 which enables it to be an eligible diffusion backing for air-cathodes (Fig. 5A and B).
255 The cathodes constructed with SSF developed an improved TPI, not only facilitating
256 the electron transfer, the proton transfer and the oxygen diffusion, but offering a large
257 surface area for ORR as well. The sequential applications of a PTFE/CB base layer
258 and PTFE DLs to the porous SSF are important for controlling the water loss from
259 anode chamber and the oxygen intrusion from outside into it. In addition, the amounts
260 of CB in the base layers serve as another significant factor that affects the
261 electrochemical performances of these SSF cathodes. As shown in Fig. 5(G), in
262 comparison with Fig. 5 (E), (F) and (H), the cathodes with CB loading of 1.56 mg
263 cm^{-2} possess more internal macropores which can enhance the interaction of protons
264 and oxygen and therefore improve the electrochemical activity of these cathodes. This

improved structure, most beneficial for the cathodic reaction, has produced the highest maximum power density (1315 ± 6 mW m^{-2}).

3.4. Resistances of electrodes

Nyquist plots of EIS operated at 0.1 V, 0 V and –0.1 V (vs. Ag/AgCl) for the cathodes were compared in Fig. 6. The inserts in Fig. 6 illustrate the high-frequency parts of the EIS for the SSF cathodes. As shown by the diminishing size of the semi-circle in Nyquist plots, the total impedance of cathodes became smaller with decreasing the applied potentials (increasing oxygen reduction overpotentials, 0.1 V → 0 V → –0.1 V), which attributed to the increasing kinetic driving force by larger overpotentials. The charge transfer resistance (R_{ct}) was obtained from the high-frequency part of the EIS spectrum in Nyquist plots while the diffusion resistance (R_d) from the low frequency part. It can be seen from the Nyquist plots that the SSF cathodes had smaller total impedances than those based on CC or SSM at all of the three polarized conditions, illustrated by the smaller semi-circles for the SSF cathodes. Moreover, the SSF cathode with CB loading of 1.56 mg cm^{-2} had the smallest total impedance.

Individual components of the internal resistance for the SSF cathodes were identified by fitting the EIS spectra to one equivalent circuit, the results of which were shown in Table 1. The R_ss of all the SSF cathodes were similar at different polarized conditions. However, the other electrochemical properties (R_{ct}, R_d and Q) varied for those cathodes with different CB loadings. The R_ds of these cathodes played a dominant role in most cases but became smaller with increasing oxygen reduction overpotential. Moreover, compared with the other cathodes, the SSF-1.56 cathodes

had the smallest R_d at each polarized condition, probably due to the optimal structure of this cathode for proton transfer and oxygen diffusion, resulting in the highest power generation. At −0.1V, for example, the SSF-1.56 cathode had the lowest R_d of 12.41 Ω, when the CB loading increased from 1.56 mg cm^{-2} to 3.12 mg cm^{-2} the R_d of SSF-3.12 cathode reached 23.26 Ω, which was attributed to the destroyed optimal structure for the oxygen diffusion. If the EIS is conducted at the same polarized condition of −0.1 V (around where most cathodes produced the maximum power densities in MFC tests (Fig. 3B)), R_d will be the largest contributor to resistance, indicating that the mass transfer is the primary limiting factor of the ORR for cathodes. Therefore it is important to increase the mass transfer by way of perturbation motion so that MFC performances can be improved. The results here were consistent with previous EIS studies, showing that the cathode diffusion resistance, larger than the charge transfer resistance, became the main part in total internal resistance of cathodes [8, 16].

Generally speaking, R_{ct} decreased with both increasing CB loadings in the base layers and increasing oxygen reduction overpotential. At polarized potential of 0.1 V, for instance, R_{ct} decreased from 11.76 Ω to 2.37 Ω as the CB loadings increased from 0.39 mg cm^{-2} to 3.12 mg cm^{-2}. Those cathodes with larger amounts of CB had lower R_{ct} values than those with lower CB loadings, the reason of which likely lay in the fact that more CB in the internal macropores of the 3D configuration improved the conductivity and thereby facilitated the electron transfer and then enhanced the overall catalytic performance of the cathodes. Besides, R_{ct} also decreased with increasing

oxygen reduction overpotential due to the larger driving force for the electron transfer.

The double layer capacitance, given that it is induced by the buildup of charge at the electrode–electrolyte interface, may has something to do with the electrode–electrolyte networks in the catalytic layer [16]. In this study, the double layer capacitance generally rose with increasing CB loadings from 0.39 mg cm^{-2} to 1.56 mg cm^{-2}, suggesting that the cathodes with higher level of CB had larger active surface areas and consequently higher catalyst utilization. The SSF-1.56 cathode, in particular, had the highest Q value, probably owing to abundant macropore in the internal structure which allowed more contact between catalyst and the open 3D porous felt. As the CB loading increased to 3.12 mg cm^{-2}, the optimal structure had been damaged, leading to a lower Q value of the SSF-3.12 cathode.

An equivalent circuit, put forward according to the flooded-agglomerate model, was used for the EIS spectra of the cathodes with CC and SSM backing, resulting in a good fit of the data to the spectra for both cathodes. Due to the poor electrical conductivity and proton transfer for the CC backing, the CC-1.56 cathode obtained the highest R_{ct} (Table 2), producing the lowest maximum power density of 820 ± 13 mW m^{-2}. Similarly, the R_{ct} value of the SSM-1.56 cathode was much higher than those of the SSF cathodes, which can be attributed to the poor proton conductivity of the SSM cathodes resulting from their flat 2D structure. At low overpotential (0.1 V), R_{ct}s for the CC and SSM cathodes were the largest contributors to the internal resistances, indicating that the ORR is primarily kinetically limited. However, when the cathodic potential was fixed at −0.1 V, some discrepancies were observed for the

two cathodes, namely, R_{ct} still being the main part of the resistance for the SSM cathode while R_d becoming the primary factor in limiting the cathodic reaction for the CC cathode.

To sum up, the cathodes with SSF backing exhibit lower internal resistance than those with CC and SSM backing, ensuring their outstanding performances in MFCs tests. On the other hand, blending CB in base layers proved to be effective for reducing the internal resistance and enhancing cathode performances in MFCs.

3.5. Corrosion

No corrosion was found on either side of the cathodes after the operation in MFCs. The composition of the metal in the SSF cathodes, which measured by SEM-EDS, showed little variation in molybdenum, chromium, iron and nickel composition before and after use in MFCs(Table 3), confirming the conclusion that power generation in MFC was not a result of corrosion of metal in SSF cathodes. In a previous study, Janicek et al[26] demonstrated that corrosion appeared on the outer surface (air facing side) of the SSM cathode during operation. The formation of insoluble iron hydroxides, which appear reddish brown or green for the SSM cathodes in their experiment, did not occur on the inner surface (water facing side) of the SSF cathodes here. The different corrosion property between the SSF herein and the SSM used in Janicek's experience probably due to the different chemical composition of the stainless steel materials.

3.6. COD removal and coulombic efficiency (CE)

COD removals, over a batch cycle of operation, ranged from 91% to 96% and the CB

loading or the type of the backing (SSF or CC or SSM) exerted no apparent effect on them. The CEs of the SSF-0.39 cathodes ranged from 13% to 35 % at the current density range of 0.7–4.0 A m^{-2} and then slightly increased when more CB was applied in the base layers (Fig. 7). The highest CE of 41% was obtained when the CB loading reached as high as 1.56 mg cm^{-2} at the current density of 5.5 A m^{-2}, but the CEs fell into the range of 14–34% with further addition of CB. Meanwhile, with the same amount of CB loading, the CEs of SSF-1.56 were obviously higher than those of CC-1.56 or SSM-1.56, fully showing the superiority of the SSF cathodes in MFC performances. It is also clear that higher CEs are achieved at increased current density, which is consistent with those results of some previous studies[7, 14]. Since increase in the current density leads to a reduction of the operation time in a batch cycle, the rise of the CE may result from the substantial decrement of oxygen that diffuses into the anode chamber. However, the values of CE obtained here were lower than those in the previous reports [6, 7], probably due to the sucrose we used as the substrate, which, being fermentable, can facilitate fermentations and/or methanogenesis, the likely competitors in the process of the electricity generation in the anode chamber.

4. Conclusions

Novel 3D macroporous air-cathodes have been built on the basis of 3D stainless steel felts, a promising alternative to CC and SSM as the air-cathode backing. MFCs equipped with this type of cathodes can produce higher power densities and CEs, which improvements we attribute to the enhanced oxygen reduction reaction at the improved three-phase interface in open 3D macroporous structure of the cathodes.

The results show that the construction of cathodes with open 3D macroporous SSF, beneficial for the applications of MFCs in a large scale, is both promising and effective for the MFC cathodes. Our experiments also demonstrate that CB blended in the base layers can improve the electrochemical properties of the cathodes, illustrated by increased current densities, reduced charge transfer resistances and diminished diffusion resistances of the cathodes. The best performance of the SSF cathodes in MFCs tests can be achieved when applied with an appropriate amount of CB of 1.56 mg cm^{-2}. In the foreseeable future, a type of high-performance SSF cathodes will advance the large scale applications of MFCs.

Acknowledgments

This work was supported by the National Natural Science Fund of China (No. 91127012 and No.21403251) and the Chinese Academy of Sciences for financial support (No. KJCX2-YW-H21).

References

1. B. E. Logan and J. M. Regan, *Environ. Sci. Technol.*, 2006, 40, 5072-5180.
2. B. E. Logan, B. Hamelers, R. Rozendal, U. Schroder, J. Keller, S. Freguia, P. Aelterman, W. Verstraete and K. Rabaey, *Environ. Sci. Technol.*, 2006, 40, 5181-5192.
3. L. Wei, H. Han and J. Shen, *Int. J. Hydrogen Energy*, 2012, 37, 12980-12986.
4. C. Fang, B. Min and I. Angelidaki, *Appl. Microbiol.Biotechnol.*, 2011, 164, 464-474.
5. S. You, Q. Zhao, J. Zhang, J. Jiang and S. Zhao, *J. Power Sources*, 2006, 162, 1409-1415.
6. F. Zhang, T. Saito, S. Cheng, M. A. Hickner and B. E. Logan, *Environ. Sci. Technol.*, 2010, 44, 1490-1495.
7. X. Zhang, S. Cheng, P. Liang, X. Huang and B. E. Logan, *Bioresour. Technol.*, 2011, 102, 372-375.
8. F. Zhang, G. Chen, M. A. Hickner and B. E. Logan, *J. Power Sources*, 2012, 218, 100-105.
9. S. Cheng and B. E. Logan, *Bioresour. Technol.*, 2011, 102, 4468-4473.
10. H. Liu, S. Cheng, L. Huang and B. E. Logan, *J. Power Sources*, 2008, 179, 274-279.
11. Y. Zuo and B. E. Logan, *Water Sci. Technol.*, 2011, 64, 2253-2258.
12. R. A. Rozendal, H. V. M. Hamelers, K. Rabaey, J. Keller and C. J. N. Buisman, *Trends Biotechnol.*, 2008, 26, 450-459.

13. H. Liu and B. E. Logan, *Environ. Sci. Technol.*, 2004, 38, 4040-4046.
14. S. Cheng, H. Liu and B. E. Logan, *Electrochem. Commun.*, 2006, 8, 489-494.
15. X. Li, X. Wang, Y. Zhang, N. Ding and Q. Zhou, *Appl. Energ.*, 2014, 123, 13-18.
16. F. Zhang, M. D. Merrill, J. C. Tokash, T. Saito, S. Cheng, M. A. Hickner and B. E. Logan, *J. Power Sources*, 2011, 196, 1097-1102.
17. J. Hou, Z. Liu, S. Yang and Y. Zhou, *J. Power Sources*, 2014, 258, 204-209.
18. P. Liu and K. Liang, *J. Mater. Sci.*, 2001, 36, 5059-5072.
19. K. Guo, B. C. Donose, A. H. Soeriyadi, A. Prévoteau, S. A. Patil, J. J. Gooding and K. Rabaey, *Environ. Sci. Technol.*, 2014, 48, 7151-7156.
20. P. Yi, L. Peng, X. Lai, M. Li and J. Ni, *Int. J. Hydrogen Energy*, 2012, 37, 11334-11344.
21. Y. Li, X. Zhang, L. Nie, Y. Zhang and X. Liu, *J. Power Sources*, 2014, 245, 520-528.
22. X. Zhang, X. Xia, I. Ivanov, X. Huang and B. E. Logan, *Environ. Sci. Technol.*, 2014, 48, 2075-2081.
23. S. Cheng, H. Liu and B. E. Logan, *Environ. Sci. Technol.*, 2006, 40, 364-369.
24. D. Lovley and E. Phillips, *Appl. Environ. Microb.*, 1988, 54, 1472-1480.
25. F. Zhang, D. Pant and B. E. Logan, *Biosens. Bioelectron.*, 2011, 30, 49-55.
26. A. Janicek, Y. Fan and H. Liu, *J. Power Sources*, 2015, 280, 159-165.

Table and figure captions

Table 1 Individual element of the cathodic internal resistances for SSF cathodes at overpotential of 0.1 V, 0 V and −0.1 V.

Table 2 Individual element of the cathodic internal resistances for CC and SSM cathodes at overpotential of 0.1 V, 0 V and −0.1 V.

Table 3 Metal composition of stainless steel felt by SEM-EDS before and after operation in MFC as cathode

Fig. 1 Equivalent circuit for (A) SSF cathodes and (B) CC and SSM cathodes

Fig. 2 Voltage generation of (A) CC, SSM and SSF cathodes with CB loading of 1.56 mg cm^{-2} and (B) SSF cathodes with different CB loading versus time, with 50 mM PBS buffer and 1.0 g L^{-1} sucrose.

Fig. 3 (A) Power densities and (B) electrode potentials of SSF cathodes with different CB loading and CC and SSM cathodes with the CB loading of 1.56 mg cm^{-2} as a function of current density (normalized to cathode projected surface area) obtained by varying the external circuit resistance (1000–50 Ω). (Error bars ± SD based on measurement of two duplicate reactors.).

Fig. 4 LSV of SSF cathodes with different CB loading and CC and SSM cathodes with the CB loading of 1.56 mg cm^{-2}.

Fig. 5 SEM images of the transversal surface of unmodified SSF (A, B) and modified cathodes with CC (C), SSM (D), SSF-0.39 (E), SSF-0.78 (F), SSF-1.56 (G), and SSF-3.12 (H).

Fig. 6 Nyquist plots of EIS spectra by six types of cathodes at polarized conditions of

0.1 V (A), 0 V (B) and −0.1 V (C) (The inserts show the EIS spectra of SSF cathodes).

Fig. 7 CEs of SSF cathodes with different CB loading and CC and SSM cathodes as a function of current density obtained by varying the external circuit resistance (1000–50 Ω).

Table 1 Individual element of the cathodic internal resistances for SSF cathodes at overpotential of 0.1 V, 0 V and −0.1 V.

Element	Overpotential	SSF-0.39	SSF-0.78	SSF-1.56	SSF-3.12
R_s(Ω)	0.1 V	15.35	15.50	13.42	15.26
	0 V	14.61	14.96	13.09	14.64
	−0.1 V	14.73	15.53	13.33	14.96
R_{ct}(Ω)	0.1 V	11.76	12.59	4.39	2.37
	0 V	10.00	4.55	1.19	2.40
	−0.1 V	9.25	9.99	2.80	1.56
R_d(Ω)	0.1 V	143.70	100.1	72.28	93.28
	0 V	53.51	84.06	37.67	51.09
	−0.1 V	31.83	34.12	12.41	23.26
Q(F)	0.1 V	0.44608	0.68286	0.7894	0.6344
	0 V	0.3713	0.33725	0.4197	0.31702
	−0.1 V	0.36619	0.34767	0.54884	0.39573

Table 2 Individual element of the cathodic internal resistances for CC and SSM cathodes at overpotential of 0.1 V, 0 V and −0.1 V.

Element	Overpotential	CC-1.56	SSM-1.56
$R_s(\Omega)$	0.1 V	24.24	23.69
	0 V	24.12	23.42
	−0.1 V	23.99	23.45
$R_{ct}(\Omega)$	0.1 V	137.7	77.44
	0 V	62.35	33.94
	−0.1 V	43.63	20.66
C_{dl} (F)	0.1 V	0.05006	0.06523
	0 V	0.04018	0.06084
	−0.1 V	0.03561	0.05359
$R_d(\Omega)$	0.1 V	108.9	16.77
	0 V	111.5	16.1
	−0.1 V	90.8	15.95
C_{ad} (F) $\times 10^{-6}$	0.1 V	4.65	3.85
	0 V	4.73	3.59
	−0.1 V	4.93	3.57

Table 3 Metal composition of stainless steel felt by SEM-EDS before and after operation in MFC as cathode

Weight percent (%)	Initial	Used
Mo	02.01	02.03
Cr	18.46	18.41
Fe	67.32	67.36
Ni	12.20	12.21

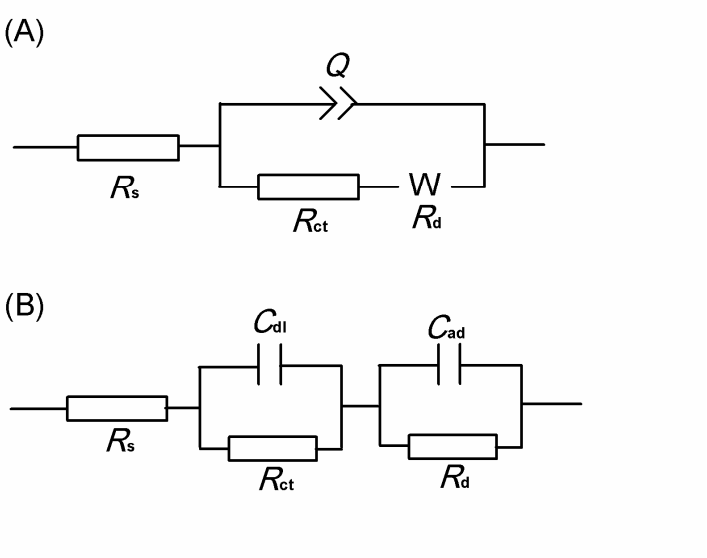

Fig. 1 Equivalent circuit for (A) SSF cathodes and (B) CC and SSM cathodes.

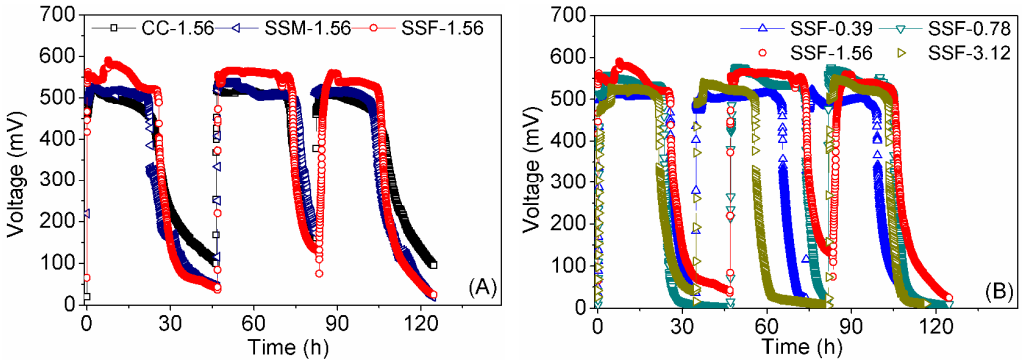

Fig. 2 Voltage generation of (A) CC, SSM and SSF cathodes with CB loading of 1.56 mg cm^{-2} and (B) SSF cathodes with different CB loading versus time, with 50 mM PBS buffer and 1.0 g L^{-1} sucrose.

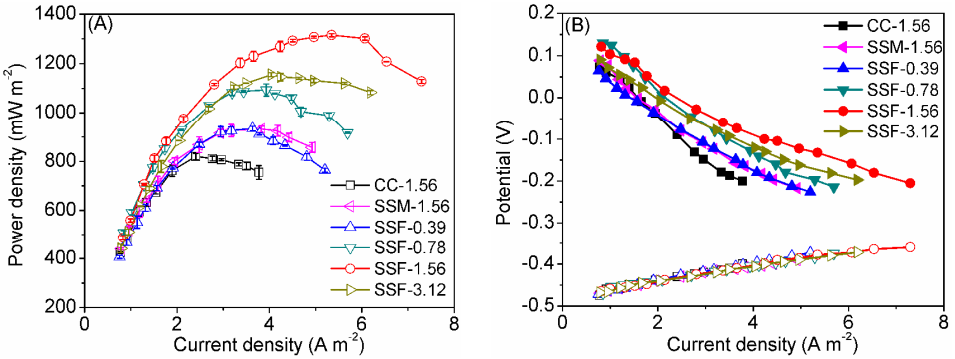

Fig. 3 Power densities (A) and electrode potentials (B) of SSF cathodes with different CB loading and CC and SSM cathodes with the CB loading of 1.56 mg cm^{-2} as a function of current density (normalized to cathode projected surface area) obtained by varying the external circuit resistance (1000–50 Ω). (Error bars ± SD based on measurement of two duplicate reactors.).

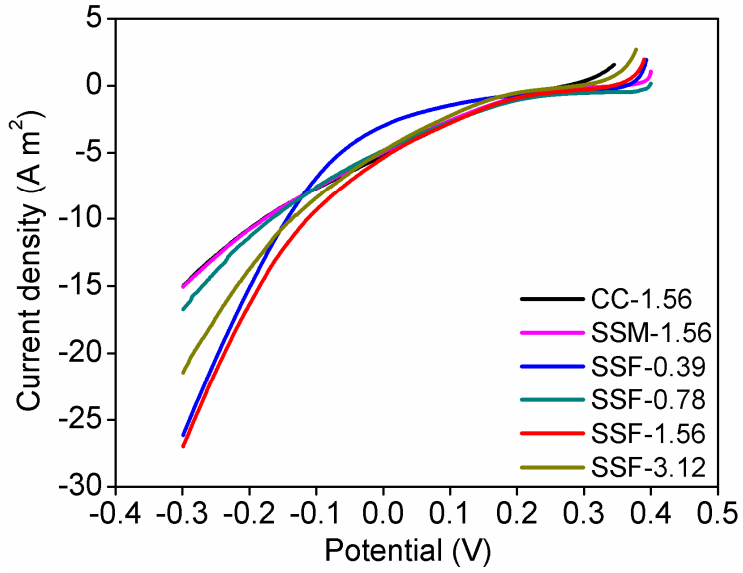

Fig. 4 LSV of SSF cathodes with different CB loading and CC and SSM cathodes with the CB loading of 1.56 mg cm^{-2}.

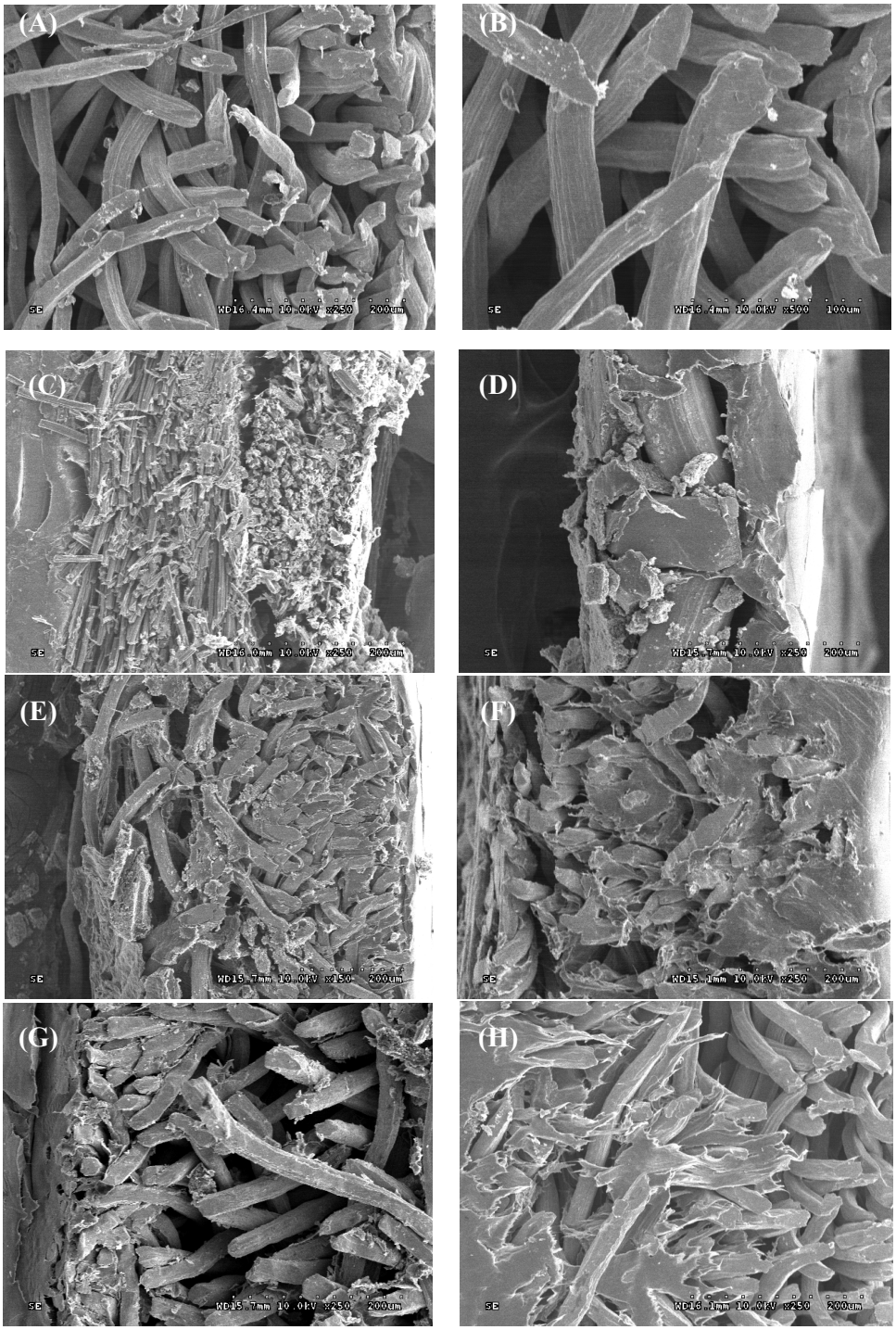

Fig. 5 SEM images of the transversal surface of unmodified SSF (A, B) and modified cathodes with CC (C), SSM (D), SSF-0.39 (E), SSF-0.78 (F), SSF-1.56 (G), and SSF-3.12 (H).

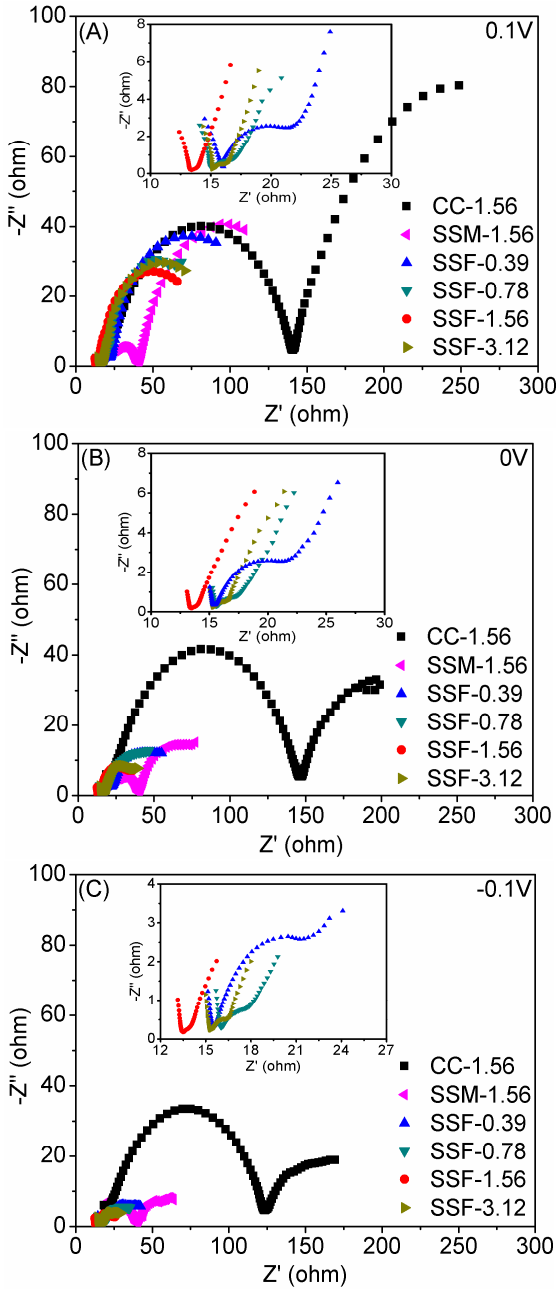

Fig. 6 Nyquist plots of EIS spectra by six types of cathodes at polarized conditions of 0.1 V (A), 0 V (B) and −0.1 V (C) (The inserts show the EIS spectra of SSF cathodes).

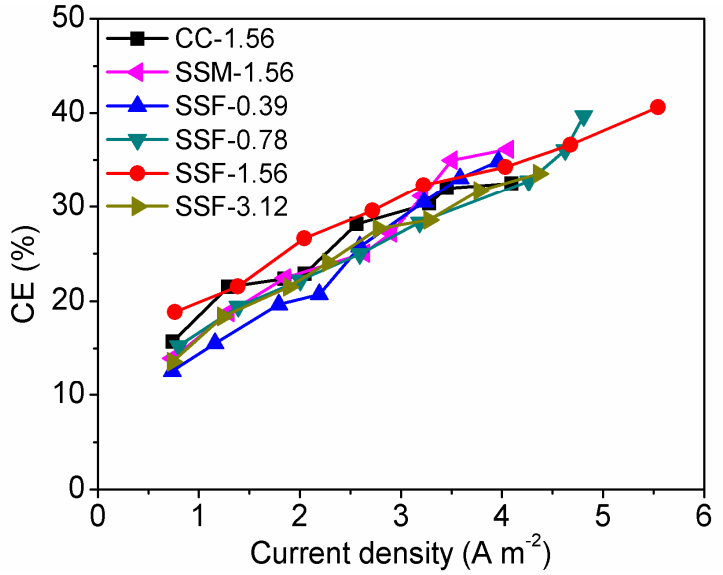

Fig. 7 CEs of SSF cathodes with different CB loading and CC and SSM cathodes as a function of current density obtained by varying the external circuit resistance (1000–50 Ω).